Catalysis Today 211 (2013) 131–136

Contents lists available at SciVerse ScienceDirect

Catalysis Today

journal homepage: www.elsevier.com/locate/cattod

Temperature influence on the reactivity of plasma species on a nickel catalyst surface: An atomic scale study

W. Somers[a,*], A. Bogaerts[a], A.C.T. van Duin[b], S. Huygh[a], K.M. Bal[a], E.C. Neyts[a]

[a] Department of Chemistry, PLASMANT Research Group, University of Antwerp, Universiteitsplein 1, B-2610 Wilrijk-Antwerp, Belgium
[b] Department of Mechanical and Nuclear Engineering, Penn State University, University Park, PA 16802, United States

ARTICLE INFO

Article history:
Received 15 December 2012
Received in revised form 4 February 2013
Accepted 8 February 2013
Available online 25 March 2013

Keywords:
Molecular dynamics simulation
Hydrocarbons
Nickel catalyst surface interactions
H_2 formation
Temperature effect
ReaxFF

ABSTRACT

In recent years, the potential use of hydrogen as a clean energy source has gained considerable attention. Especially H_2 formation by Ni-catalyzed reforming of methane at elevated temperatures is an attractive process. However, a more fundamental knowledge at the atomic level is needed for a full comprehension of the reactions at the catalyst surface. In this contribution, we therefore investigate the H_2 formation after CH_x impacts on a Ni(1 1 1) surface in the temperature range 400–1600 K, by means of reactive molecular dynamics (MD) simulations using the ReaxFF potential. While some H_2 formation is already observed at the lower temperatures, substantial H_2 formation is only obtained at elevated temperatures of 1400 K and above. At 1600 K, the H_2 molecules are even the most frequently formed species. In direct correlation with the increasing dehydrogenation at elevated temperatures, an increased surface-to-subsurface C-diffusivity is observed as well. This study highlights the major importance of the temperature on the H_2 formation.

1. Introduction

Steam methane reforming over a supported nickel catalyst has been a widely used process for hydrogen production for several decades [1]. Because of the potential use of hydrogen as a source of clean energy, there is a continuous interest in this process, but further improvements regarding the efficiency are clearly required to warrant the economic viability. Sehested [1] discussed this issue and summarized the most important challenges of the steam methane reforming process, namely: maintaining the catalyst activity and reducing carbon formation, sintering, and sulfur poisoning. Complementary to the substantial experimental research that has already been carried out, a more fundamental knowledge at the atomic level is needed.

Experimental studies until now mainly focused on the adsorption and decomposition of methane on Ni-catalysts [2–4]. The dissociative adsorption of CH_4 on Ni(1 1 1) was studied with HREELS [2], SIMS and XPS [3,4]. Furthermore, in order to obtain a full description of the reactions and the reaction barriers at the atomic scale, a number of computational studies were performed as well. Density functional theory (DFT) calculations illustrated the higher adsorption and dissociation probability of CH_4 molecules on Ni(1 0 0) and on stepped structures compared to Ni(1 1 1) [5,6]. Additionally, the complete successive dehydrogenation of CH_4 has been recently discussed, also based on DFT calculations [7]. While DFT calculations are very accurate, and suitable for small systems, classical molecular dynamics (MD) simulations are capable of describing the atomic interactions for larger systems, and on a longer timescale. Mueller et al. employed such simulations to study the dissociation of methyl radicals on nickel surfaces as a function of temperature. These authors found a higher reactivity of Ni(1 0 0) and a stepped surface compared to a flat Ni(1 1 1) surface [8]. Although it is found that Ni(1 1 1) is not the most reactive surface, it is still the subject of a lot of research, since it is the most abundant facet in typical nickel catalysts [9–11].

Such research is not only interesting from a pure catalytic point of view, but also for plasma-catalytic applications. This technology is an alternative for improving the conventional steam methane reforming process, since it combines the high reactivity of a plasma with the high selectivity of a catalyst [12,13]. The influence of a plasma on the reactivity was demonstrated by Nozaki, demonstrating that vibrationally excited methane improved the dissociative chemisorption on nickel surfaces [14,15]. Although synergistic effects have been demonstrated before [16], the exact mechanisms of the interactions of the plasma species at the catalyst surface remain unclear [17]. Such interactions are also of importance for the growth of nanostructures, such as carbon nanotubes (CNTs), for which nickel catalysts are also used in combination with plasma technology [18,19]. During the plasma-enhanced chemical vapor deposition of CNTs, precursors such as CH_4, CH_3 and H_2 are used

* Corresponding author. Tel.: +32 3 265 23 82; fax: +32 3 265 23 43.
E-mail address: wesley.somers@ua.ac.be (W. Somers).

0920-5861/$ – see front matter © 2013 Elsevier B.V. All rights reserved.
http://dx.doi.org/10.1016/j.cattod.2013.02.010

[20]. MD simulations of the interactions of these precursors on the catalyst surface can provide information regarding the initial mechanisms. Previously, MD simulations were performed in combination with Monte Carlo techniques to study other aspects of the growth of CNTs, such as the influence of the electric field [21].

In our previous work [22], we used molecular dynamics to simulate single and consecutive impacts of CH_x radicals on four different nickel surfaces, namely Ni(1 1 1), Ni(1 0 0) and two stepedged Ni(1 1 1) surfaces, at a temperature of 400 K, which is typical for cold (i.e., non-thermal equilibrium) atmospheric pressure plasmas. In agreement with previous findings [5,6,8], we observed a higher reactivity on Ni(1 0 0) and the stepped surfaces, and elucidated the different reaction mechanisms occurring on the different surfaces. Furthermore, some H_2 molecules were formed, although the fraction at this temperature was very small. However, it can be expected that the probability of H_2 formation increases at higher temperature, which has been suggested before [7].

In this work, we have increased the temperature to the region of the so-called warm plasmas [23–25], i.e. 1000–2000 K, in order to determine the temperature onset for H_2 formation. For instance, in the transitional regime of a gliding arc discharge, the non-equilibrium properties of low-temperature plasmas are maintained, while the gas temperature is slightly increased. This leads to an increase in the number of excited species, which, as mentioned above, leads to an enhanced dissociation. Furthermore, the increased gas temperature might also improve the reactivity of the catalyst, and thus create a synergistic effect. In the first part of this contribution, we compare the results of consecutive CH_x impacts at 400 K on Ni(1 1 1) employing the Bussi thermostat [26] and the Berendsen thermostat [27], in order to verify the equivalence of both methods to study this system. We specifically verify the equivalence of both thermostats in simulating this system, in order to demonstrate the validity of the comparison between the results obtained in this work and in our previous work. In the second part, consecutive CH_x impacts are performed in a temperature range from 800 to 1600 K, again on the Ni(1 1 1) surface, with the focus on H_2 formation.

2. Computational details

2.1. Interatomic potential and thermostat

Reactive molecular dynamics (MD) simulations are performed, based on the Reactive Force Field (ReaxFF) potential [28] to derive the forces between the atoms, using parameters developed by Mueller and coworkers [8]. Furthermore, these authors validated the accuracy of the parameter set by comparison of a large number of hydrocarbon reactions on nickel surfaces with quantum mechanics calculations. Moreover, the same force field has also been used to simulate the growth of CNTs in close agreement with experiments [29–31]. ReaxFF is based on the bond order/bond distance relationship introduced by Abell [32]. The total system energy is the sum of multiple partial energy terms, related to pair interactions, lone electron pairs, atomic under- and overcoordination, valence and torsion angles, conjugation and hydrogen bonding. Furthermore, van der Waals and Coulomb interactions are also included, so that not only covalent bonds are described, but also non-bonded interactions between all atoms. Charge distributions are calculated with the electron equilibration method [33], which is based on the geometry and connectivity of the system. A more detailed description of the force field can be found elsewhere [34].

Upon impact on the substrate, the impinging particles exchange a part of their kinetic energy with the nickel surface atoms. In the microcanonical (NVE) ensemble, the total energy of the system remains constant throughout the simulated impact. This ensemble was used in our previous simulations [22]. After each impact, however, the surface needed to be re-equilibrated at 400 K prior to each new impact. For this re-equilibration, we used the Berendsen thermostat [27], in which the velocities are rescaled at each time step in order to enforce the desired temperature (i.e., the total kinetic energy) of the system. However, although the Berendsen thermostat allows control of the simulated system's temperature, it does not generate the true canonical (NVT) ensemble.

Bussi et al. proposed another thermostat which, similar to the Berendsen thermostat, also rescales the atomic velocities using a certain scaling factor depending on the current and desired temperature of the system [26]. It differs from the Berendsen thermostat in the way the scaling factor is calculated. Whereas the Berendsen formalism relies on a simple deterministic function to obtain the rescaling factor during each time step, Bussi's approach is a stochastic procedure where the rescaling factor is randomly sampled from a specified distribution. In contrast to the Berendsen thermostat, this thermostat is able to correctly generate the canonical ensemble, and is therefore used in this work.

The simulations in this work are intended to capture the dynamics of the system, and do not necessarily capture the correct thermodynamics. In this respect, however, it should be noted that we specifically focus on the short timescale dynamic phenomena, such as adsorption and desorption. In order to capture the thermodynamics of the system, a different simulation method would be required. For this purpose, we plan to use the Grand Canonical Monte Carlo method in our further research.

2.2. Simulation method

The studied Ni(1 1 1) surface consists of 300 atoms equally divided over 6 atomic layers. Prior to the consecutive impacts, the surface is first equilibrated at the desired temperature using the Bussi thermostat with a coupling constant of 100 fs, in the range 400–1600 K, with a 200 K interval. In order to simulate an semi-infinite surface, periodic boundary conditions are applied in the $\{x,y\}$ directions.

The impacting species are CH_x radicals ($x = \{1,2,3\}$), which are added to the system at a z position of 10 Å above the top layer of the nickel surface. The initial $\{x,y\}$ coordinates and the initial velocity vector are randomized. Each impact is followed for 6.25 ps, in which the radicals can be adsorbed, decomposed or reflected. In the case of reflection, the radicals are removed from the system. The resulting surface is subsequently used as the input configuration for the next impact. This sequence is repeated 150 times for the CH_3 impacts, and 250 times for the CH_2 and CH impacts. The lower number of simulated CH_3 impacts is due to fact that after 150 impacts there are no more adsorptions or reactions on the surface, while in the case of CH_2 and CH, more impacts are needed for saturation to occur. After this number of impacts, clear trends in the reactivity after impact are observed. For each case, i.e., the sequence of impacts of each species at the six different temperatures, three different simulations were performed and the results reported here are the averages over these three simulations with the associated standard deviations. Thus, in total, 54 simulations were carried out, accounting for a total of 11,700 impacts.

It is essential to keep in mind that these simulations approach the effect of plasma on a catalyst through the reactivity of the radicals. Experimentally, this increases the concentration of active species near the catalyst surface and can enhance the energy efficiency. It is also important to realize, however, that not all possible effects of plasma on the catalyst can be described in these simulations. For instance, the influence of electrons, and therefore the electron density, on carbon deposition through direct electron impact dissociation of methane cannot be taken into account in our simulations. This process would effectively and drastically reduce

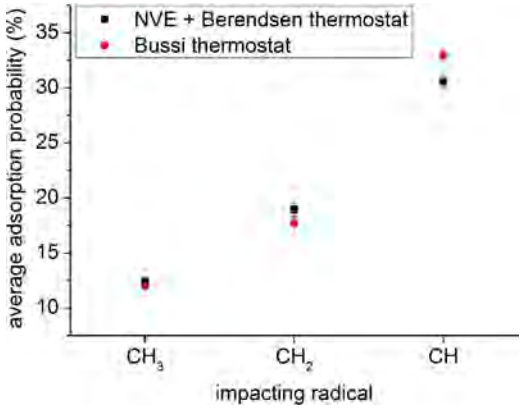

Fig. 1. Comparison of the average adsorption probabilities and associated standard deviations of the CH_x radicals on Ni(1 1 1) as determined from NVE simulations in combination with the Berendsen thermostat and NVT simulations employing the Bussi thermostat.

the catalytic activity. However, note that the electron density of the transitional regime of a gliding arc discharge is 10^{12} cm^{-3}, while the typical value in a DBD is around 10^{14}–10^{15} cm^{-3} [25,35]. Furthermore, in the transitional regime of a gliding arc discharge Te ≈ 1 eV, which is a characteristic value for non-thermal plasmas. Since the electron energy is comparable for DBD and gliding arc discharges (in the transitional regime), and the electron density is lower for the latter discharge, we expect that the temperature will have the most substantial influence on a process such as carbon deposition.

Additionally, the plasma might alter the reactivity of the catalyst by changing the crystallinity. As discussed in our previous work [22], the type of nickel surface indeed influences the reactivity after impacts of plasma species. For this purpose, our next study will further focus on the reactivity on several nickel surfaces, ranging from polycrystalline to amorphous structures.

3. Results and discussion

3.1. Comparison of the Berendsen and Bussi thermostats

Both the adsorption probability and the reactions after adsorption as obtained from the simulations with the Bussi thermostat are compared with our previous results, which were obtained from simulations under the NVE ensemble in combination with the Berendsen thermostat [22]. As shown in Fig. 1, the average adsorption probability after 150 consecutive CH_3 impacts is almost equal for both methods, with only a small difference of less than 0.5% between the two values. The difference between the average adsorption probabilities obtained with both methods slightly increases for the CH_2 impacts, i.e. up to 1%. However, when considering the standard deviations on these averages, both methods still give very similar results. Only in the case of the consecutive CH impacts, there is a noticeable difference between the average adsorption probabilities obtained with both methods, even though it remains low (3%). The progressing adsorption probability after each consecutive impact is determined by the reactivity of the incoming radical, i.e. the number of free radical electrons, as well as by the steric hindrance induced by the radicals which are already adsorbed on the surface. Since the reactivity of the incoming radicals does not change during the simulations, the difference between the adsorption probabilities obtained using both methods can be allocated to the different steric hindrance of the nickel surface and its adsorbed species toward the incoming radicals. The types of adsorbed species are determined by the reactions after adsorption, in which new non-adsorbed species are formed. These reactions involve the breaking of C—H bonds of the adsorbed radicals, and thus, result in adsorbed species with less H-atoms, such as CH radicals and C-atoms. The latter species present a lower steric hindrance compared to CH_3 or CH_2 radicals adsorbing on the surface. A comparison between the average numbers of formed non-adsorbed species in both simulation methods can therefore assist in further studying the small difference in the adsorption probabilities.

The reactions after the adsorption of CH_3 radicals are very rare, resulting in only 2 broken C—H bonds on a total of 150 impacts for both methods. Both bond breaking events subsequently lead to the formation of 2 CH_4 molecules. Since the reactivity is found to be equal for both methods, the resulting nickel surfaces will strongly resemble each other; hence, the adsorption probability of CH_3 is similar for both methods, as discussed above. The type of non-adsorbed species formed after CH_2 and CH impacts is the same for the simulations with the Berendsen and Bussi thermostat, as shown in Fig. 2. Especially for the formation of CH_4 and CH_3 species, the differences are very small. Even for the formation of CH_2 species there is only a limited influence of the thermostat, such that the resulting nickel surfaces will not differ significantly, and therefore, adsorption probabilities within the same range are expected.

The results above show that although the simulated ensemble is different, the use of the Bussi thermostat and the Berendsen thermostat in combination with NVE simulations result in the same reactivity of small hydrocarbons on a Ni(1 1 1) surface.

3.2. Temperature effect

3.2.1. H_2 formation

It is important to point out that in our previous simulations, at a temperature of 400 K, no H_2 formation was observed after CH_x

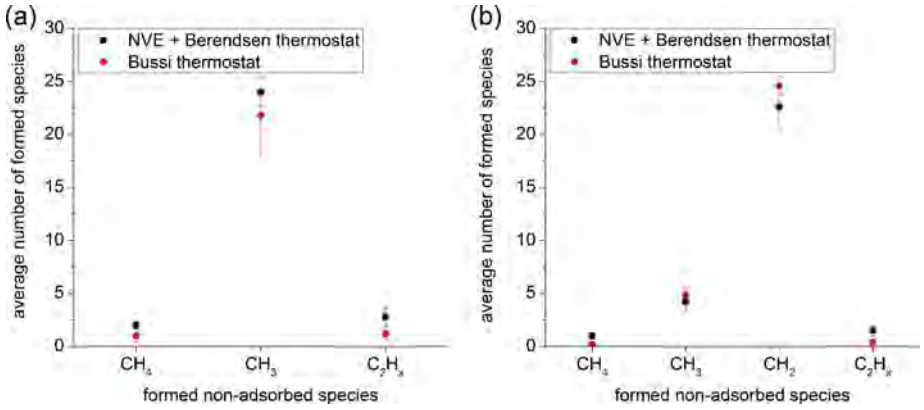

Fig. 2. Comparison between the average number of species formed and associated standard deviations, after 250 consecutive impacts of (a) CH_2 and (b) CH radicals.

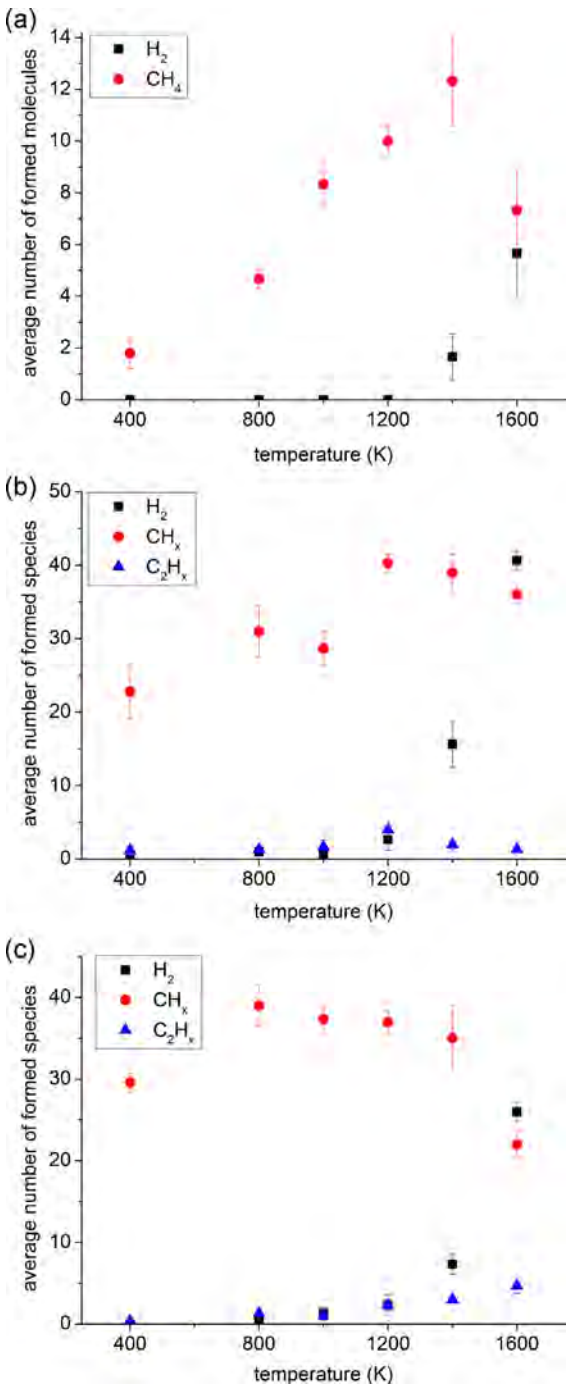

Fig. 3. Average number of formed species, and associated standard deviations, as a function of temperature after (a) 150 consecutive CH_3 impacts, (b) 250 consecutive CH_2 impacts and (c) 250 consecutive CH impacts.

impacts on Ni(1 1 1) [22]. On other nickel surfaces, only a small amount of H_2 was formed at the same temperature. So it is essential to know if H_2 formation can occur after CH_x impacts on Ni(1 1 1), and, if so, what the threshold temperature of this reaction is.

3.2.1.1. CH_3 impacts. After 150 consecutive CH_3 impacts on Ni(1 1 1), no H_2 formation is observed up to a temperature of 1200 K (see Fig. 3a). It has been demonstrated by Mueller [7] that adsorbed CH_3 is kinetically stable on Ni(1 1 1) at low temperatures, and that higher temperatures are required to overcome the barrier for C—H bond breaking (0.80 eV). This is also observed in our simulations, where the number of broken C—H bonds, and thus the number of CH_4 molecules formed is increasing as a function of temperature. This implies that the impacting radicals have enough energy to abstract a H-atom from the adsorbed species or from the nickel surface. However, the recombination of two hydrogen atoms to form H_2 still requires too much energy. Our simulation results indicate that a temperature of 1400 K is required for this barrier to be overcome, with an average of 2 H_2 molecules formed on a total of 150 impacts. The H_2 formation further increases to nearly 6 molecules on a total of 150 impacts, when increasing the temperature to 1600 K. This means that 4% of the CH_3 impacts are followed by H_2 formation. Additionally, there is a decrease in the number of CH_4 molecules formed, since the H-atoms adsorbed on the nickel surface now recombine into H_2.

3.2.1.2. CH_2 impacts. Even at 400 K, the reactivity of CH_2 and CH was found to be much higher than the CH_3 reactivity, giving rise to the formation of CH_4, reflected CH_3 and CH_2, and a small fraction of C_2 species. The species formed after 250 consecutive CH_2 and CH impacts can be divided into 3 groups: H_2, CH_x and C_2H_x species. As illustrated in Fig. 3b, a low number of H_2 molecules is formed at 800 K, 1000 K and 1200 K upon the CH_2 impacts. However, this number increases significantly at temperatures of 1400 K and 1600 K, up to 41 H_2 molecules for the latter temperature, thus 16% of the CH_2 impacts is followed by H_2 formation. This is even higher than the number of CH_x species formed, in contrast to the results at lower temperatures, where the number of CH_x species is larger than that of H_2. Furthermore, this result is in agreement with previous research on thermal methane cracking [36], where a temperature of more than 1600 K was needed to generate H_2 as the main component of the evolving gas. At temperatures up to 1200 K, most of the surface-bound H-atoms react with the impacting radicals to form CH_x species. In some rare occasions, the H-atoms have enough energy to recombine into H_2. As is also the case for the CH_3 impacts, this process is activated at a temperature of 1400 K, and at even higher temperatures most H-atoms are found to recombine, thus causing a reduction in the number of CH_x species formed. The energy barrier for the recombination of 2 H-atoms to H_2 is calculated with the nudged elastic band (NEB) method [37], and is found to be 1.66 eV. This is higher than the calculated barrier for H-diffusion over the nickel surface, which we calculated as 0.35 eV. The increase in temperature is thus essential for crossing the energy barrier for H_2 formation. Additionally, some C_2H_x species are formed, although their formation is hardly influenced by the temperature.

3.2.1.3. CH impacts. The H_2 formation due to CH impacts (Fig. 3c) is initiated at 800 K. As is the case for the CH_2 impacts, a significant increase in the H_2 formation is observed at temperatures of 1400 K and 1600 K. Furthermore, the trend concerning the number of CH_x species formed as a function of the temperature is maintained. Indeed, at the lower temperatures, the CH_x species are the most occurring species, while at 1600 K, the H_2 molecules are the dominant species formed. At this temperature, 12% of the CH impacts are followed by H_2 formation, corresponding to an average of 30 H_2 molecules formed after 250 consecutive impacts. This is lower than the number of H_2 molecules formed due to CH_2 impacts, as can be expected since there are less H-atoms in the CH-system. The stability of H-atoms on Ni(1 1 1) has been investigated by Mueller [7]. It was found that at low temperatures, most hydrogen atoms are adsorbed on the surface, since the energy for chemisorption is −0.59 eV per H. However, at higher temperatures the adsorbed H-atoms tend to recombine to H_2, as is the case in our simulations. In contrast to the results of the CH_2 impacts, the C_2H_x formation is slightly dependent on the temperature, although the C_2H_x fraction remains small. Furthermore, the ionization energy of these species is lower than that of CH_x species, i.e. 11.56 eV for C_2H_6 versus

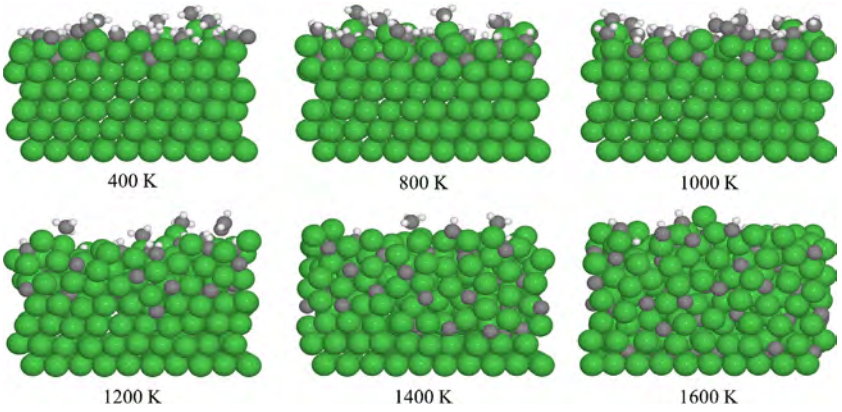

Fig. 4. Side view of the Ni(1 1 1) surface after 250 consecutive CH_2 impacts at different temperatures. The green spheres correspond to the nickel atoms, the gray spheres to the C-atoms and the white spheres to the H-atoms. (For interpretation of the references to color in this figure legend, the reader is referred to the web version of the article.)

12.98 eV for CH_4 [38]. This implies that, in a plasma-catalytic process, the C_2H_x species are more likely to decompose in the plasma after they are formed at the catalyst surface than the more stable CH_x species. The easier decomposition of these species in a plasma, as a function of residence time, has already been demonstrated in the literature [39].

Under experimental conditions corresponding to the simulation results, the H_2 formation occurs at temperatures that may lead to sintering of the catalyst. This increases the size of the nickel particles, and decreases the activity due to the reduced catalytic surface area [1]. It should be noted that in our simulations, sintering and thus this loss of catalytic surface area is not included, since we study the interactions on a semi-infinite surface. It is thus important to remark that while the total catalytic surface area may indeed be reduced at these temperatures (i.e. in the order of 1400 K), this simulated substantial H_2 formation corresponds to highly localized small-area surface patches.

3.2.2. Carbon diffusion into the nickel surface

The results discussed above indicate the positive effect of increasing the temperature on the H_2 formation. However, the temperature also influences the diffusion of the carbon atoms into the nickel surface, which is not a desired effect. Indeed, in the steam methane reforming process, carbon deposition can reduce the performance of the catalyst, for example by blocking the active sites of the catalyst. As mentioned above, the reactivity in the case of the CH_3 impacts is rather low, especially when comparing these results with the reactivity of the other impacting radicals. Only a few CH_3 radicals become fully dehydrogenated after adsorption, and consequently, the resulting C-atoms can diffuse into the nickel surface. Up to 1400 K, the C-atoms only diffuse into the first subsurface layer, but at a temperature of 1600 K, the diffusion goes deeper into the nickel structure, i.e., until the third subsurface layer.

The same effect is also observed for the dehydrogenated C-atoms originating from CH_2 and CH impacts. Little diffusion, i.e., in the range of 16 diffused C-atoms on a total of 250 CH_2 impacts, is observed up to temperatures of 1000 K, while more extensive diffusion, i.e., in the range of 91 diffused C-atoms, occurs at a temperature of 1600 K. Since many C—H bonds are broken to form H_2, the number of dehydrogenated C-atoms is much higher than in the case of CH_3 impacts, where 24 C-atoms diffused into the nickel surface after 150 CH_3 impacts. Fig. 4 illustrates the carbon diffusion into the nickel surface for CH_2 impacts at various temperatures. It is observed that the C-atoms only diffuse to the first subsurface layer up to a temperature of 1000 K. At higher temperatures, the C-atoms can reach lower-lying Ni-layers. The same is observed for the diffusion after the CH impacts, indicating that the C-atoms gain enough energy to diffuse to lower layers. The energy barrier for the diffusion of a C-atom from the μ_3 hcp site to an octahedral site in the first subsurface layer is calculated with the NEB method, and is found to be 1.16 eV. This is significantly lower than the energy required for further diffusion into the surface. For instance, the diffusion from an octahedral site in the first subsurface layer to a tetrahedral site in the second subsurface layer requires 2.76 eV. The same type of diffusion from the third to the fourth subsurface layer also needs a similar amount of energy, namely 2.26 eV. Thus, as observed in Fig. 4, high temperatures are required to overcome the energy barrier of diffusion to lower subsurface layers. The diffusion pathways of C-atoms on a Ni(1 1 1) surface have been extensively investigated by Abild-Pedersen [40]. It was found that for the diffusion of a C-atom from the top layer of a clean surface to the first subsurface, an energy of about 1.00 eV was needed, which is in agreement with our findings.

The results discussed above show that an optimal operating condition is at a temperature around 1400 K, since at higher temperatures, the diffusion of C-atoms into the nickel surface becomes too dominant, and at lower temperatures the H_2 formation is too limited. A similar general conclusion was reached by Nikoo and Amin [41]. These authors concluded that a high temperature (>1173 K) was required for the optimal production of syngas (H_2 + CO) during the dry reforming of methane. Furthermore, Nozaki [14] discussed the dominance of thermal reactions on the catalyst surface at temperatures exceeding 973 K. Such thermal activation is also observed in our results. Note that in these studies also oxidative species were present, such as H_2O or CO_2, in contrast to our simulations. These species will oxidize the adsorbed C-atoms, and release them from the surface as CO. In combination with the H_2 formation, this is the general mechanism for syngas production during steam methane reforming. In future work, we plan to perform MD simulations for a full description at the atomic level of the steam methane reforming process.

4. Summary and conclusions

The influence of the temperature on the reactivity of CH_x species on a Ni(1 1 1) surface was investigated using reactive molecular dynamics simulations, with a specific emphasis on H_2 formation.

First, we compared the use of two different ensembles for the simulation of this system, viz. the microcanonical ensemble in combination with the Berendsen thermostat, and the canonical Bussi thermostat, to validate the comparison with our previous results. It is demonstrated that there are no significant differences in the results as obtained from both methods, indicating that the obtained

processes and mechanisms are not sensitive to the exact temperature control method.

Second, it is shown that H_2 formation can occur after CH_x impacts on Ni(1 1 1) at sufficiently high temperatures. The reactivity toward H_2 formation is the lowest in the case of the CH_3 impacts. Only at a temperature of 1400 and 1600 K, the system has sufficient energy to cross the barrier of 1.66 eV for the recombination of 2 H-atoms into a H_2 molecule. At lower temperatures, the H-atoms react with the impacting CH_3 radicals to form CH_4. The same high temperatures of 1400 K and 1600 K are also required to obtain a significant amount of H_2 formation after CH_2 and CH impacts. Again, at lower temperatures, most surface-adsorbed H-atoms will react with the impacting species, instead of forming H_2. At 1600 K, about 4%, 16% and 12% of the CH_3, CH_2 and CH impacts, respectively, are followed by H_2 formation.

Finally, it is also illustrated, in agreement with experimental observations, that the high temperatures do not only lead to an increase in the H_2 formation, but also promote the diffusion of C-atoms into the subsurface region of the crystal. At temperatures of 1400 K and 1600 K, the diffusion barrier to lower subsurface layers can be overcome, reducing the possibility to oxidize the adsorbed C-atoms into CO, if oxidative species are present. Overall, the results imply that an optimal temperature for an efficient H_2 formation on Ni(1 1 1) lies around 1400 K. At higher temperatures, the diffusion of C-atoms into the nickel surface becomes overly dominant, while at lower temperatures the H_2 formation is too limited. The temperature of 1400 K is reached in warm plasmas, which are also characterized by the high number of reactive excited species. Therefore, a synergistic effect might be obtained, which makes it an interesting technology for the methane reforming process.

This study further elucidates the importance of the temperature on the methane reforming process, which is an important step toward efficient H_2 formation as a source of clean energy.

Acknowledgments

This work was carried out using the Turing HPC infrastructure at the CalcUA core facility of the Universiteit Antwerpen (UA), a division of the Flemish Supercomputer Center VSC, funded by the Hercules Foundation, the Flemish Government (department EWI) and the UA.

References

[1] J. Sehested, Catalysis Today 111 (2006) 103–110.
[2] M.B. Lee, Q.Y. Yang, S.L. Tang, S.T. Ceyer, Journal of Chemical Physics 85 (1986) 1693.
[3] Q.Y. Yang, K.J. Maynard, A.D. Johnson, S.T. Ceyer, Journal of Chemical Physics 102 (1995) 7734.
[4] M.P. Kaminsky, N. Winograd, G.L. Geoffroy, M. Albert Vannice, Journal of the American Chemical Society 108 (1986) 1315–1316.
[5] B. Xing, X.-Y. Pang, G.-C. Wang, Z.-F. Shang, Journal of Molecular Catalysis A: Chemical 315 (2010) 187–196.
[6] J. Li, E. Croiset, L. Ricardez-Sandoval, Journal of Molecular Catalysis A: Chemical 365 (2012) 103–114.
[7] J.E. Mueller, A.C.T. van Duin, W.A. Goddard, Journal of Physical Chemistry C 113 (2009) 20290–20306.
[8] J.E. Mueller, A.C.T. van Duin, W.A. Goddard, Journal of Physical Chemistry C 114 (2010) 4939–4949.
[9] K.-M. Kang, H.-W. Kim, I.-W. Shim, H.-Y. Kwak, Fuel Processing Technology 92 (2011) 1236–1243.
[10] Q. Feng, T. Li, H. Yue, K. Qi, F. Bai, J. Jin, Applied Surface Science 254 (2008) 2262–2268.
[11] X. Guo, Y. Sun, Y. Yu, X. Zhu, C.-J. Liu, Catalysis Communications 19 (2012) 61–65.
[12] H.L. Chen, H.M. Lee, S.H. Chen, Y. Chao, M.B. Chang, Applied Catalysis B 85 (2008) 1–9.
[13] A.-J. Zhang, A.-M. Zhu, J. Guo, Y. Xu, C. Shi, Chemical Engineering Journal 156 (2010) 601–606.
[14] T. Nozaki, N. Muto, S. Kado, K. Okazaki, Catalysis Today 89 (2004) 57–65.
[15] T. Nozaki, N. Muto, S. Kadio, K. Okazaki, Catalysis Today 89 (2004) 67–74.
[16] X. Tu, J.C. Whitehead, Applied Catalysis B 125 (2012) 439–448.
[17] H.K. Song, J.-W. Choi, S.H. Yue, H. Lee, B.-K. Na, Catalysis Today 89 (2004) 27–33.
[18] K. Ostrikov, U. Cvelbar, A.B. Murphy, Journal of Physics D: Applied Physics 44 (2011) 174001.
[19] K. Ostrikov, Reviews of Modern Physics 77 (2005) 489–511.
[20] R.M. Sankaran, Journal of Physics D: Applied Physics 44 (2011) 174005.
[21] E.C. Neyts, A.C.T. van Duin, A. Bogaerts, Journal of the American Chemical Society 134 (2012) 1256–1260.
[22] W. Somers, A. Bogaerts, A.C.T. van Duin, E.C. Neyts, Journal of Physical Chemistry C 116 (2012) 20958–20965.
[23] A. Gutsol, A. Rabinovich, A. Fridman, Journal of Physics D: Applied Physics 44 (2011) 274001.
[24] M.S. Yaghmaee, B. Shokri, N.H. Khiabani, A. Sarani, Plasma Processes and Polymers 6 (2009) S631–S636.
[25] A. Fridman, S. Nester, L.A. Kennedy, A. Saveliev, O. Mutaf-Yardimci, Progress in Energy and Combustion Science 25 (1999) 211–231.
[26] G. Bussi, D. Donadio, M. Parrinello, Journal of Chemical Physics 126 (2007) 014101.
[27] H.J.C. Berendsen, J.P.M. Postma, W.F. van Gunsteren, A. Di Nola, J.R. Haak, Journal of Chemical Physics 81 (1984) 3684.
[28] A.C.T. van Duin, S. Dasgupta, F. Lorant, W.A. Goddard, Journal of Physical Chemistry A 105 (2001) 9396–9409.
[29] E.C. Neyts, Y. Shibuta, A.C.T. van Duin, A. Bogaerts, ACS Nano 4 (2010) 6665–6672.
[30] E.C. Neyts, A.C.T. van Duin, A. Bogaerts, Journal of the American Chemical Society 133 (2011) 17225–17231.
[31] E.C. Neyts, K. Ostrikov, Z.J. Han, S. Kumar, A.C.T. van Duin, A. Bogaerts, Physical Review Letters 110 (2013) 065501.
[32] G.C. Abell, Physical Review B 31 (1985) 6184–6196.
[33] W.J. Mortier, S.K. Ghosh, S. Shankar, Journal of the American Chemical Society 108 (1986) 4315–4320.
[34] K. Chenoweth, A.C.T. van Duin, W.A. Goddard, Journal of Physical Chemistry A 112 (2008) 1040–1053.
[35] A. Fridman, Plasma Chemistry, first ed., Cambridge University Press, New York, 2008.
[36] A. Abánades, E. Ruiz, E.M. Ferruelo, F. Hernández, A. Cabanillas, J.M. Martínez-Val, J.A. Rubio, C. López, R. Gavela, G. Barrera, C. Rubbia, D. Salmieri, E. Rodilla, D. Gutiérrez, International Journal of Hydrogen Energy 36 (2011) 12877–12886.
[37] G. Henkelman, H. Jónsson, Journal of Chemical Physics 113 (2000) 9987.
[38] Q. Wang, B.-H. Yan, Y. Jin, Y. Cheng, Plasma Chemistry and Plasma Processing 29 (2009) 217–228.
[39] D.H. Lee, K.-T. Kim, M.S. Cha, Y.-H. Song, International Journal of Hydrogen Energy 35 (2010) 10967–10976.
[40] F. Abild-Pedersen, J.K. Nørskov, J.R. Rostrup-Nielsen, J. Sehested, S. Helveg, Physical Review B 73 (2006) 115419.
[41] M.K. Nikoo, N.A.S. Amin, Fuel Processing Technology 92 (2011) 678–691.